Appl. Phys. B (2015) 121:307–313
DOI 10.1007/s00340-015-6230-x

Applied Physics B
Lasers and Optics

Electron density measurements using high-order harmonic generation in laser-produced plasmas

R. A. Ganeev[1] · M. Suzuki[1] · S. Yoneya[1] · H. Kuroda[1]

Received: 26 April 2015 / Accepted: 20 September 2015 / Published online: 1 October 2015

Abstract We demonstrate the method of the measurements of electron density in the low-dense, low-ionized laser-produced plasma using the nonlinear optical process of high-order harmonic generation of ultrashort pulses at the conditions of the quasi-phase-matching of driving and harmonic waves. Electron density was defined using the relations of quasi-phase-matching. We show the results of our measurements of electron density in the range of 10^{16}–10^{17} cm^{-3} using the multi-jet silver plasma produced for the harmonic generation.

1 Introduction

The electron density of plasma governs various properties of this medium. Several diagnostic methods were developed for the measurements of electron density, which include Langmuir probe [1, 2], Thomson scattering [3], laser interferometry [4], and plasma spectroscopy [5–11]. Latter method is the most frequently used technique, which is based on the analysis of the Stark broadening of spectral lines [12, 13]. However, in the case of this method, three additional broadening mechanisms (Doppler broadening, pressure broadening, and instrumental broadening) may contribute to line broadening during laser ablation. The difficulty in definition of the role of various factors increases the uncertainty in the accuracy of the measurements of electron density in the region of low densities of plasma. Note that most of above methods were developed for the analysis of relatively dense (10^{18} cm^{-3} and higher) and strongly ionized plasmas. As for the low-density (10^{16}–10^{17} cm^{-3}) low-ionized plasmas, the Stark broadening of ionic lines will be of the order of 0.005 nm, which is hard to distinguish from other spectral broadening mechanisms. In the meantime, such plasmas are of special interest, since they allow the efficient conversion of the long-wavelength laser sources towards the short-wavelength spectral region.

In this paper, we demonstrate the method of electron density measurements using the nonlinear optical frequency conversion in the laser-produced plasmas. We generate the high-order harmonics of ultrashort pulses in the laser-produced plasmas at the conditions of the quasi-phase-matching of driving and harmonic waves and define the electron density of plasma through the relations of quasi-phase-matching.

2 Description of method

Quasi-phase-matching is one of the methods for resolving the phase mismatch problem during high-order harmonic generation of ultrashort laser pulses in various media. The phase mismatch in plasma is related to the dephasing between harmonic and driving waves. The difference in the velocities of these waves leads to the conditions when, at some distance from the beginning of the medium, the phase shift between the waves becomes close to π. After propagation of this distance (coherence length, $L_{coh} = \pi/\Delta k$, where Δk is the difference between the wave vectors of driving and harmonic pulses), the constructive accumulation of harmonic photons reverts to the destructive one. At these conditions, the newly generated coherent extreme ultraviolet photons being in reverse phase compensate the earlier generated photons, thus decreasing the harmonic yield.

✉ R. A. Ganeev
rashid_ganeev@mail.ru

[1] Ophthalmology and Advanced Laser Medical Center, Saitama Medical University, Saitama 350-0495, Japan

The quasi-phase-matching allows diminishing this restriction of harmonic conversion efficiency by different means [14]. Particularly, the quasi-phase-matching was demonstrated by using the multiple gas puffs [15–18]. Recently, the implementation of quasi-phase-matching in laser-produced plasmas using the ablation of targets by spatially modulated heating pulses was reported [19].

Here we demonstrate the method of the measurements of electron density based on the analysis of the coherence length of the group of enhanced harmonics generated in the laser-produced plasmas at the conditions of quasi-phase-matching. Quasi-phase-matching aims at cancelling the out-of-phase emission, particularly, by modulating the medium density [20], which allows suppression of the phase mismatch between the interacting waves. One can accomplish this suppression by dividing the whole extended plasma onto a group of small plasma jets. Various methods could be used to divide the extended laser-produced plasma. Among them are (1) the interference of two heating beams on the target surface with the variable angle between the interacting beams, (2) tilting of the multi-slit shield placed on the path of heating pulse, and (3) installation of the multi-slit shield inside the telescope on the path of heating pulses. The most affordable methods are (2) and (3) since they allow the tuning of jet sizes by simple tilting or relocation of the multi-slit shield.

There are four main factors that contribute to the phase mismatch between the driving and harmonic waves: atomic and ionic dispersion, Gouy phase shift, intensity-dependent dynamic phase shift, and electron-affected plasma dispersion [21]. The first one refers to the variation in the refractive index of the neutrals and ions, which shows considerably less influence than the dispersion-induced by the presence of free electrons (fourth factor) in the plasma. This assumption allows excluding the influence of atom- and ion-induced dispersion on the phase mismatch. Gouy phase shift could also be dismissed in the case of loosely focused driving pulses when the confocal parameter of the focused radiation exceeds the sizes of plasma. This assumption corresponds to our experimental conditions (16 and 5 mm, respectively). The Gouy phase mismatch [22] in our case was in the range of 0.2–0.7 cm^{-1} depending on plasma conditions. The laser intensity used to calculate dynamic atomic phase shift is related to the barrier suppression ionization [23, 24]. The saturation intensity for silver ions was calculated to be 1×10^{14} W cm^{-2}. The phase mismatch between the harmonics emitted at different parts of 5-mm-long plasma medium was estimated to be in the range of 5–10 cm^{-1}. Finally, the phase mismatch due to plasma electrons was considerably larger (of the order of ~100 cm^{-1} for the thirties harmonics) compared with other components [25]. Thus, at the used conditions, the only factor influencing phase mismatch is related to the presence of electrons in the laser-produced plasmas.

The plasma dispersion-induced phase mismatch for the qth harmonic is defined by the relation

$$\Delta k_{\text{disp}} = qN_e e^2 \lambda / 4\pi m_e \varepsilon_0 c^2, \quad (1)$$

where λ is the wavelength of driving radiation, N_e is the electron density, m_e and e are the mass and the charge of the electron, c is the light velocity, and ε_0 is the vacuum permittivity [26, 27]. The coherence length of this harmonic is

$$L_{\text{coh}} = \pi / \Delta k \approx \pi / \Delta k_{\text{disp}} = 4\pi^2 m_e \varepsilon_0 c^2 / q N_e e^2 \lambda. \quad (2)$$

From this expression, the coherence length (measured in millimetres) at the conditions of using the 800-nm driving laser could be presented as

$$L_{\text{coh}} \approx 1.4 \times 10^{18} / \left(N \times q_{\text{qpm}}\right). \quad (3)$$

Here q_{qpm} is the harmonic order in the quasi-phase-matching region showing the highest enhancement and N is the electron density in the plasma jets measured in cm^{-3}. This simple formula allows defining the electron density by knowing the coherence length, which is length of single jet at the conditions of quasi-phase-matching in the multi-jet plasma, and the maximally enhanced harmonic order. The decrease in heating pulse fluence should lead to the decrease in electron density and tuning of q_{qpm} towards the shorter-wavelength region. Similarly, one can anticipate that, for the plasma jets of different sizes, the maximally enhanced harmonics will also be generated in different parts of the extreme ultraviolet spectrum. These assumptions allow the comparison of electron density measurements using different multi-jet plasmas and different ablation conditions. The proposed method of electron density measurements could be a useful tool for analysis of the electrons appearing on the path of the driving pulses during laser ablation of targets.

3 Experimental set-up for harmonic generation in the multi-jet plasmas

The uncompressed radiation of Ti:sapphire laser was used as a heating pulse (central wavelength $\lambda = 802$ nm, pulse duration 370 ps, pulse energy up to 4 mJ, 10-Hz pulse repetition rate) to ablate the target for plasma formation. The laser radiation was propagated through the spatial filter consisted of two lenses (L_1 and L_2, Fig. 1) and pinhole to improve the spatial profile and increase the sizes of laser beam. The growth of laser beam sizes is necessary for irradiation of the target using the homogeneous line-shaped beam. The heating pulses were focused using the 200-mm

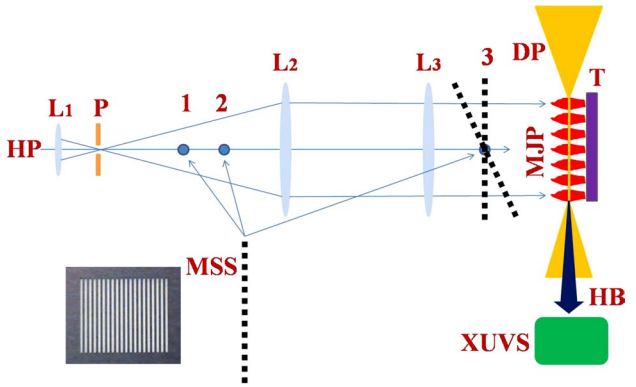

Fig. 1 Experimental set-up for the high-order harmonic generation using the formation of variable multi-jet plasmas in the focal plane of cylindrical lens (L_3) at different positions (*1–3*) of the multi-slit shield. L_1, L_2, lenses of telescope; P, pinhole of telescope; T, silver target; MSS, multi-slit shield; HP, heating pulse; DP, driving pulse; HB, harmonic beam; MJP, multi-jet plasma; XUVS, extreme ultraviolet spectrometer. *Inset* image of multi-slit shield

focal length cylindrical lens (L_3) inside the vacuum chamber containing an ablating material to create the homogeneous extended plasma plume above the target surface. The intensity of heating pulses on a plain target surface was varied in the range of 1×10^9–4×10^9 W cm^{-2}. Silver was used as the ablating target due to excellent properties of Ag plasma as the efficient medium for harmonic generation along the extreme ultraviolet region. The length of this target was 5 mm.

The compressed driving pulse from the same laser with the energy of up to 3 mJ and 64-fs pulse duration was used, 42 ns from the beginning of plasma ablation, for harmonic generation in the plasma plume. The driving pulse was focused using the 400-mm focal length spherical lens in the extended plasma from the orthogonal direction as shown in Fig. 1. The confocal parameter of the focused radiation was 16 mm. The intensity of driving pulse in the focus area was varied up to 1×10^{15} W cm^{-2}. The harmonic emission was analysed by an extreme ultraviolet spectrometer containing a gold cylindrical mirror and a 1200 grooves/mm flat-field grating with variable line spacing. The spectrum of harmonics was recorded by a micro-channel plate detector with the phosphor screen, which was imaged onto a CCD camera.

The modulation of the spatial shape of heating pulse was accomplished using the installation of the multi-slit shield on the path of propagation of this radiation. The image of multi-slit shield is shown in the inset in Fig. 1. The sizes of each slit of this shield were 0.3 mm, and the distance between the slits was 0.3 mm. The images of plasma formations were captured from the top of the vacuum chamber by a CCD camera. Figure 2a shows the line and multi-jet plasmas formed on the silver surface by the extended

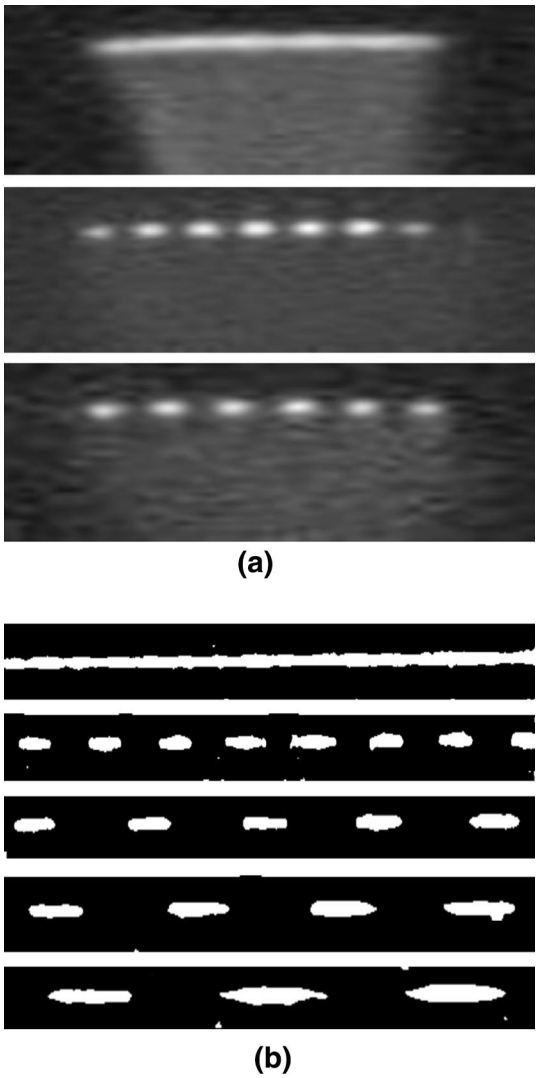

Fig. 2 **a** Images (from *top to bottom*) of extended, seven-jet, and six-jet plasmas formed on the silver target. **b** Images of the ablated surface of silver target during formation of (from *top to bottom*) extended line-shaped plasma produced without the use of multi-slit shield, and eight-, five-, four-, and three-jet plasmas produced by placing the multi-slit shield in different positions inside the telescope

focused heating beam and by installation of the multi-slit shield at different positions inside the telescope. One can see the extended, seven-, and six-jet plasma structures. The sizes of plasma jets were defined by measurement of the ablated areas of silver target (Fig. 2b), rather than by measurement of the images of plasma emission. In the latter case, the registered emission of plasma does not accurately correspond to the actual sizes of jets. The jet sizes were also calculated from the geometrical characteristics of the radiation propagated through the multi-slit shield placed at different positions inside the telescope. The gradual tilting of the multi-slit shield placed at the position 3 (Fig. 1) allowed the steady growth of the number of jets up to 14.

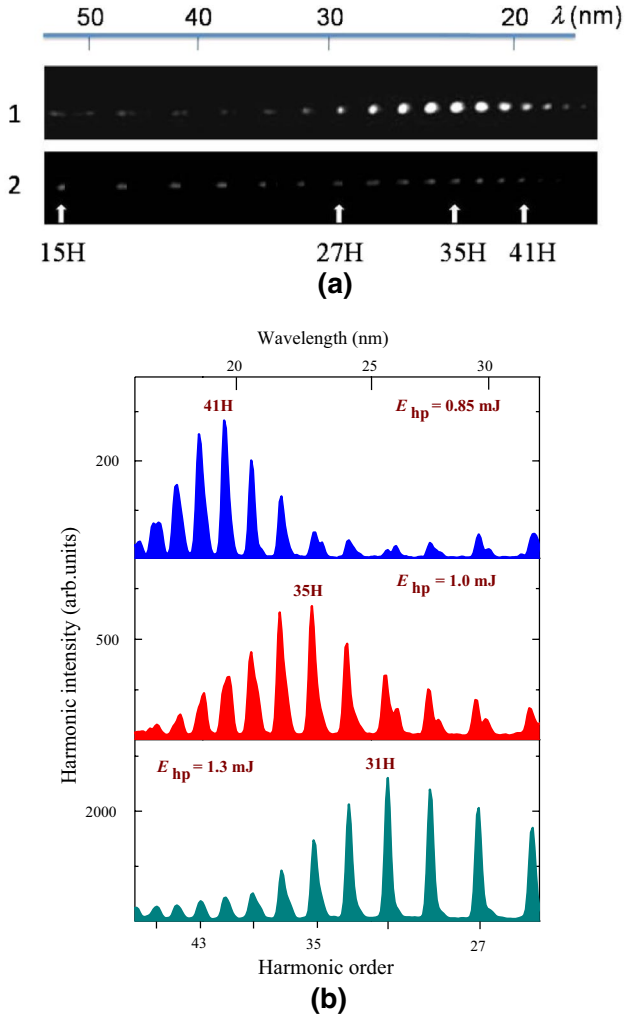

Fig. 3 **a** Raw images of harmonic spectra obtained from the five-jet plasma (*panel 1*) and extended (5-mm-long) homogeneous plasma (*panel 2*). **b** Harmonic spectra obtained from the five-jet plasma formed on the silver target at different energies of the heating pulses

4 Measurements of electron density

The harmonic spectrum from the 5-mm-long Ag plasma in the case of removal of the multi-slit shield from the path of heating radiation showed a featureless plateau-like shape (Fig. 3a, panel 2). This pattern of harmonic spectrum was dramatically changed once we introduced the multi-slit shield inside the telescope (panel 1). One can see a significant enhancement of a group of harmonics in the 18- to 30-nm spectral range. The two raw images of harmonic spectra shown in Fig. 3a were taken by moving the multi-slit shield in and out of the path of heating pulse, without any other changes of experimental conditions. Note that, in the latter case, the whole length of plasma was two times longer. The enhancement factor of the 35th harmonic from the five 0.5-mm-long plasma jets produced by the 1-mJ heating pulses was ~20× compared with the same harmonic generated in the extended plasma. The quasi-phase-matching conditions were also fulfilled, to some extent, for some other nearby harmonics. These spectra demonstrate the enhancement of a few harmonics, rather than single one, due to small dispersion of the low-dense plasma.

The harmonic spectra from the silver ablation using three different energies of heating pulses are shown in Fig. 3b in the case of the five 0.5-mm-long plasma jets. The energies shown in Fig. 3b (0.85, 1.0, 1.3 mJ) account for the pulse energies measured after propagation of the heating radiation through the multi-slit shield. The energies of pulses before irradiation of multi-slit shield were two times larger. One can clearly see the quasi-phase-matching-induced enhancement of the groups of harmonics, which were tuned depending on the energy of heating pulses. We observed this enhancement at shorter wavelengths while using lesser excitation of target (Fig. 3b; compare the spectral maxima of quasi-phase-matching-enhanced harmonics at different energies of heating pulses). The ablation of silver target using weaker and stronger beams led to the shift of the maximally enhanced harmonics from the 41st order towards the 31st one.

Equation (3) allows the definition of electron density in those three cases by measuring the q_{qpm} at the same sizes of plasma jets. The electron density was calculated to be 7×10^{16} cm^{-3} in the case of 0.5-mm-long jets and at the maximally enhanced harmonics centred near the 41st order (Fig. 3, heating pulse energy 0.85 mJ). The excitation of target using stronger heating pulses (1.0 and 1.3 mJ) led to the plasma formation contained larger amount of electrons (with the electron density calculated to be 8×10^{16} and 9×10^{16} cm^{-3}, respectively). These studies showed the dependence of the electron density on the heating pulse energy.

Below we present our electron density studies using variable sizes of the jets formed on the target surface. Figure 4 shows three spectra of plasma harmonics obtained using six 0.4-mm-long, five 0.5-mm-long, and three 0.8-mm-long plasma jets. No any other changes were introduced during these experiments excluding the movement of the multi-slit shield along the telescope axis, thus maintaining a similar fluence of heating pulse on the target surface. In each of these cases, we observed the enhancement of the groups of harmonics in different spectral ranges. The maximum enhancements were observed for the 25th, 35th, and 43rd harmonics in the cases of the 0.8-, 0.5-, and 0.4-mm-long plasma jets, respectively. The electron density of plasma in these three cases was the same due to equal fluency of the heating pulse on the target surface. The calculation of electron density confirmed the equality of electron density in these three cases within the accuracy of measurements (7.0×10^{16}, 8.0×10^{16}, 8.1×10^{16} cm^{-3}, respectively)

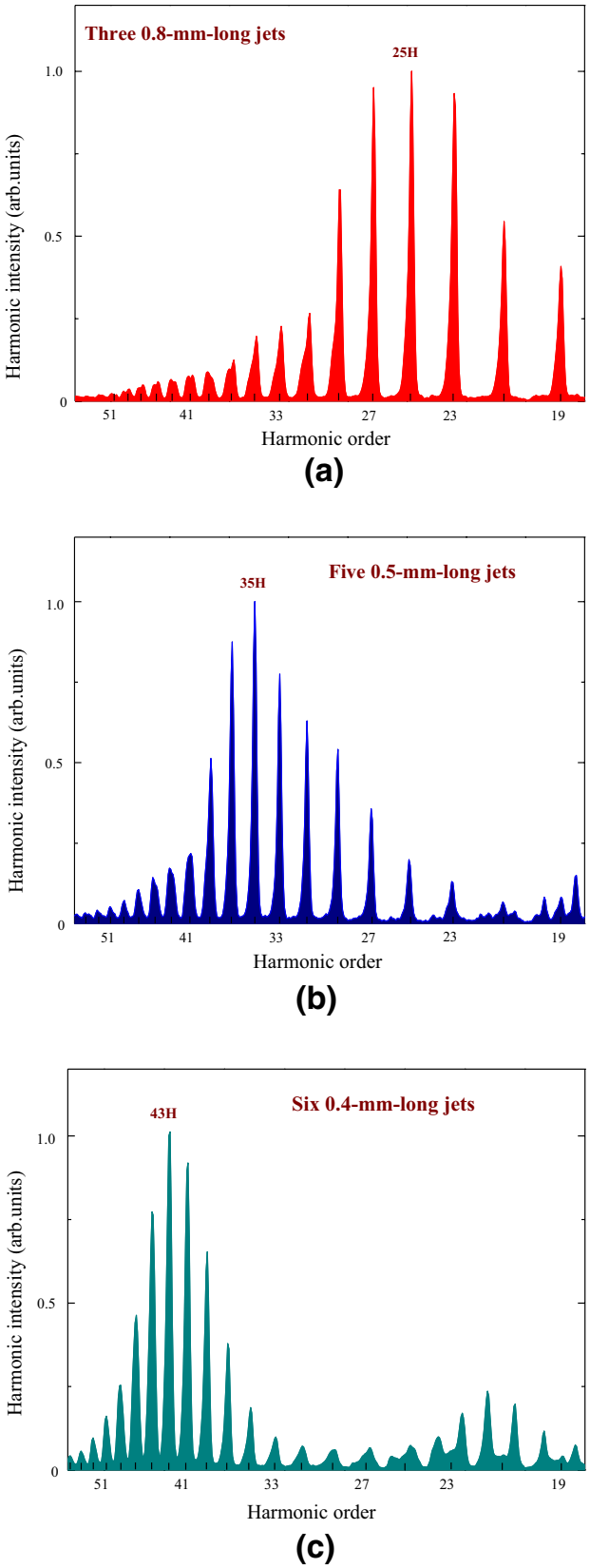

assuming the experimentally measured parameters of L_{coh} and q_{qpm}.

◀**Fig. 4** Normalized harmonic spectra in the cases of different multi-jet plasmas. The sizes of jets are **a** 0.8 mm, **b** 0.5 mm, and **c** 0.4 mm. The delay between heating and driving pulses is maintained at 42 ns. The fluence of heating pulse in the target surface is 0.5 J cm^{-2}. The intensity of driving pulse in plasma area is 9 × 10^{14} W cm^{-2}. The driving pulse is propagated at the distance of 100 μm above the target surface

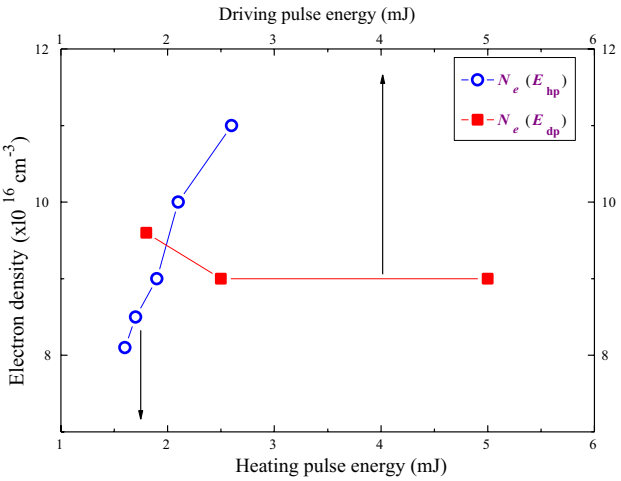

Fig. 5 Variations of electron density of laser-produced plasma at different energies of heating (*empty circles*) and driving (*filled squares*) pulses

Note that the electrons interacting with the driving and harmonic waves comprise those produced during the initial formation of plasma and those appeared during ionization of neutrals and singly charged ions by the propagating driving pulse. Independently, on the role of these groups of electrons in the phase mismatch, the proposed technique allows the measurement of the instant amount of electrons.

To compare the influence of the driving and heating pulses on the electron density, we show these dependences on a single plot. The calculations of electron densities were accomplished using Eq. (3). The growth of the tunnelling ionization cross section leading to the appearance of additional free electrons in the multi-jet medium did not spoil the conditions of quasi-phase-matching. Figure 5 (filled squares) shows the near similarity of the electron density along a broad range of variations of the driving pulse energy. One can see that the threefold growth of driving pulse energy (from 1.85 to 5 mJ) did not significantly change the electron density. A different pattern was observed once we changed the heating pulse energy, which led to variation of the electron density of plasma at the conditions of multi-jet structure formation (Fig. 5, empty circles). The comparative studies of the harmonic spectra generated from the eight-jet silver plasma at different fluences of heating 370-ps pulses on the target surface were accomplished by changing the energy of heating radiation using the calibrated filters. We

varied the energy of heating pulse to analyse the influence of this parameter on the dynamics and shape of the envelope of harmonic distribution using the same multi-jet plasma. The group of harmonics gradually tuned towards the lower orders (i.e. longer-wavelength region) with the growth of the heating pulse energy. It is seen that the N_e was strongly dependent on the variation of the heating pulse energy. Solid lines are inserted for better viewing of the influence of heating and driving pulse energies on the electron density. A decrease in electron density at weaker excitation of the target should lead to optimization of the quasi-phase-matching for higher q_{qpm} to keep the product $q_{qpm} \times N_e$ unchanged at the fixed spatial characteristics of plasma jets [see Eq. (3)]. Thus, the additional electrons appearing during stronger ablation of targets significantly influence the quasi-phase-matching conditions. However, whether these additional electrons were attributed to those produced during either ablation or tunnel ionization of additional silver particles remains unclear.

The accuracy of the proposed method is defined by the uncertainty in definition of strongest harmonic order and by the uncertainty in the measurements of plasma sizes. Shot-to-shot measurements of quasi-phase-matching-induced spectra from multi-jet plasmas showed that the highest yield was obtained for the same harmonic order. The accuracy in the measurement of the spatial characteristics of plasma jets mostly depended on the uncertainty in the relation between the sizes of the ablated spot on the target surface and the density distribution for each plasma jet. We assumed that, after propagation through the shield, each component of modulated heating beam had a rectangular shape with the sizes equal to the sizes of the slit of multi-slit shield. The accuracy of electron density measurements was mostly defined by the accuracy of the measurements of plasma jet sizes (± 0.1 mm) and by definition of the maximally enhanced harmonic (± 1). Based on above assumptions, the error of the measurements of electron density was estimated to be 20 %. It is difficult to compare the accuracy of this method with other reported methods due to different ranges of electron densities. Note that all plasma and electron diagnostic methods have accuracy issues and none of them are perfect. Each of them has merits and demerits, since the accuracy of those methods depends on the experimental conditions.

There are a few other uncertainties in the behaviour of electron cloud during spreading out of surface. In particular, little is known about the relative distribution of electrons and other particles in the plasma plume. Whether the distribution of electron density along the plasma plume remains same as the distribution of other components at the later stage of plasma formation remains unknown. Note that our measurements show the influence of electrons on the nonlinear optical process in the plasma plume and define their density at the fixed spot inside the plume, while not defining their spatial distribution. To measure the spatial distribution of electrons, one has to gradually move the driving pulse out of the ablating surface.

5 Conclusions

Among the advantages of the quasi-phase-matching of plasma harmonics are the simplicity in regulation of electron density in the multi-jet plasmas, the high enhancement factors of harmonics, and the availability of the express analysis of electron density. Two former advantages were demonstrated in previous studies [19, 28, 29]. The reported conversion efficiency for the enhanced 33rd harmonic of Ti:sapphire laser ($\lambda \approx 24$ nm) generated in the Ag plasma jets ($\sim 2 \times 10^{-5}$) [19] is among the highest values achieved so far in this spectral region during high-order harmonic generation in both gases and plasmas. Regarding latter advantage, the definition of maximally enhanced harmonics at the fixed sizes of separated plasma jets allows the calculation of electron density, as it was demonstrated in present studies. The electron density was defined using the relations of quasi-phase-matching. The proposed method allows the analysis of the variations of electron density in the low-ionized plasmas. Particularly, the variation of the distance from ablating target and the delay between heating and driving pulses will allow analysing the dynamics of electron density along the low-ionized medium.

References

1. D.H. Lowndes, D.B. Geohegan, A.A. Puretzky, D.P. Norton, C.M. Rouleau, Science **273**, 898 (1996)
2. E. de Posada, J.G. Lunney, M.A. Arronte, L. Ponce, E. Rodríguez, T. Flores, *Journal of Physics: Conference Series*, vol. 274 (2011), p. 012079
3. S.B. Cameron, M.D. Tracy, J.P. Camacho, IEEE Trans. Plasma Sci. **24**, 45 (1996)
4. T. Mochizuki, K. Hirata, H. Ninomiya, K. Nakamura, K. Maeda, S. Horiguchi, Y. Fujiwara, Opt. Commun. **72**, 302 (1989)
5. S.S. Harilal, C.V. Bindhu, R.C. Issac, V.P.N. Nampoori, C.P.G. Vallabhan, J. Appl. Phys. **82**, 2140 (1997)
6. F.J. Gordillo-Vázquez, A. Perea, J.A. Chaos, J. Gonzalo, C.N. Afonso, Appl. Phys. Lett. **78**, 7 (2001)
7. S.S. Harilal, B. O'Shay, M.S. Tillack, J. Appl. Phys. **98**, 013306 (2005)
8. R. Sanginés, C.S. Aké, H. Sobral, M. Villagrán-Muniz, Phys. Lett. A **367**, 351 (2007)
9. B. Verhoff, S.S. Harilal, J.R. Freeman, P.K. Diwakar, A. Hassanein, J. Appl. Phys. **112**, 093303 (2012)
10. N. Smijesh, R. Philip, J. Appl. Phys. **114**, 093301 (2013)
11. M. Ruiz, F. Guzmán, M. Favre, S. Hevia, N. Correa, H. Bhuyan, E.S. Wynham, H. Chuaqui, *Journal of Physics: Conference Series*, vol. 511, (2014), p. 012064
12. H.R. Griem, *Plasma Spectroscopy* (McGraw-Hill, New York, 1964)

13. H.R. Griem, *Spectral Line Broadening by Plasmas* (Academic Press, New York, 1974)
14. A. Bahabad, M.M. Murnane, H.C. Kapteyn, Nat. Photonics **4**, 570 (2010)
15. J. Seres, V.S. Yakovlev, E. Seres, C.H. Streli, P. Wobrauschek, C.H. Spielmann, F. Krausz, Nat. Phys. **3**, 878 (2007)
16. A. Pirri, C. Corsi, M. Bellini, Phys. Rev. A **78**, 011801 (2008)
17. V. Tosa, V.S. Yakovlev, F. Krausz, New J. Phys. **10**, 025016 (2008)
18. A. Willner, F. Tavella, M. Yeung, T. Dzelzainis, C. Kamperidis, M. Bakarezos, D. Adams, M. Schulz, R. Riedel, M.C. Hoffmann, W. Hu, J. Rossbach, M. Drescher, N.A. Papadogiannis, M. Tatarakis, B. Dromey, M. Zepf, Phys. Rev. Lett. **107**, 175002 (2011)
19. R.A. Ganeev, M. Suzuki, H. Kuroda, Phys. Rev. A **89**, 033821 (2014)
20. P.L. Shkolnikov, A. Lago, A.E. Kaplan, Phys. Rev. A **50**, R4461 (1994)
21. H. Singhal, V. Arora, B.S. Rao, P.A. Naik, U. Chakravarty, R.A. Khan, P.D. Gupta, Phys. Rev. A **79**, 023807 (2009)
22. F. Lindner, G.G. Paulus, H. Walther, A. Baltuska, E. Goulielmakis, M. Lezius, F. Krausz, Phys. Rev. Lett. **92**, 113001 (2004)
23. P. Salieres, A. L'Huillier, P. Antoine, M. Lewenstein, Adv. At. Mol. Opt. Phys. **41**, 83 (1999)
24. Y. Tamaki, J. Itatani, M. Obara, K. Midorikawa, Phys. Rev. A **62**, 063802 (2000)
25. H. Singhal, R.A. Ganeev, P.A. Naik, V. Arora, U. Chakravarty, P.D. Gupta, J. Appl. Phys. **103**, 013107 (2008)
26. A. Paul, R.A. Bartels, R. Tobey, H. Green, S. Weiman, I.P. Christov, M.M. Murnane, H.C. Kapteyn, S. Backus, Nature **421**, 51 (2003)
27. L. Zheng, X. Chen, S. Tang, R. Li, Opt. Express **15**, 17985 (2007)
28. R.A. Ganeev, M. Suzuki, H. Kuroda, J. Phys. B At. Mol. Opt. Phys. **47**, 105401 (2014)
29. R.A. Ganeev, V. Tosa, K. Kovács, M. Suzuki, S. Yoneya, H. Kuroda, Phys. Rev. A **91**, 043823 (2015)